CHARACTERIZATION OF URINARY IRON LOSS IN THE *fsn* (FLAKY SKIN) ANEMIA MOUSE MUTANT

By

ROBERT LEE KRESS

BS, Birmingham-Southern College, 2008

Submitted to the graduate degree program in Clinical Research and the Graduate Faculty of the University of Kansas in partial fulfillment of the requirements for the degree of Master of Science.

_____

Chairperson Edward F. Ellerbeck, M.D., MPH

_____

Robert A. White, Ph.D.

_____

Flavia C. Costa, Ph.D.

Date Defended: June 26th, 2014

The Thesis Committee for ROBERT LEE KRESS

certifies that this is the approved version of the following thesis:

CHARACTERIZATION OF URINARY IRON LOSS IN THE *fsn* (FLAKY SKIN) ANEMIA MOUSE MUTANT

_____

Chairperson Edward F. Ellerbeck, M.D., MPH

Date approved: July 7th, 2014

Abstract

Iron overloading is a serious medical problem for blood transfusion-dependent diseases such as sickle cell disease, β-Thalassemia Major, and Myelodysplastic syndromes which require chronic blood transfusions to treat their related sequelae. Alternative treatment options to iron chelation therapy are currently lacking. The goal of this study was to identify a mechanism in a mouse model with the unique ability to excrete excess iron through urine and can uncover a novel pharmaceutical target to treat iron overload. The flaky-skin anemia (*fsn*) mouse possesses a mutation in the *Ttc7* gene (tetratricopeptide repeat domain 7) and had been observed to excrete elevated iron levels in its urine. We hypothesized that the mutation in *fsn* results in decreased transferrin-bound iron reabsorption in the kidney, resulting in elevated iron excretion in the urine. While the mechanism of high iron excretion in *fsn* mice remains unknown, we have ruled out the possibility of transferrin-bound iron leak from the kidney. *fsn* kidney cells not only expressed TfR1 (transferrin receptor-1) on the surface, but were capable of endocytosing transferrin-bound iron. Additionally, Cubilin and Megalin, known transferrin receptors, mRNA levels were not significantly different between *fsn* and WT littermate kidneys. However, we have detected lower levels of *Dmt1* mRNA in the *fsn* kidney. Further work should focus on DMT1 protein expression in the nephron and investigate whether DMT1 (divalent metal transporter-1) protein levels impact the pathogenesis observed in the *fsn* anemia mouse mutant.

Acknowledgements

I would like to thank my mentor, Dr. Robert White, for his guidance over this year. I am thankful for the trust and confidence you had in me. I will take away many lessons from my time in your lab and without a doubt it has made me a better scientist.

I would also like to thank Dr. Flavia Costa and Dr. Chris Theisen whom I have had the privilege of working with this year. Your support and knowledge has helped me not only in this project but further in my career.

Table of Contents

Abstract ..... **iii**
Acknowledgements ..... **iv**
Table of Contents ..... **v**
List of Tables and Figures ..... **vi**
Introduction **1**
Materials and Methods **5**
Ethics Statement 5
Mice 5
High Iron Diet 5
Quantitative real-time PCR (qRT-PCR) 5
Flow Cytometry 7
Western Blotting of Kidney Samples and Antibodies 7
Transferrin ELISA and Iron Measurement in Urine Samples 8
Urine Electrophoresis 9
Statistics 9
Results **10**
Iron transport gene expression 10
Transferrin receptor 1 & Transferrin uptake flow cytometry 11
Endosomal protein markers in the kidney 12
qRT-PCR on TTC7a and Transferrin endocytosis related genes 13
Urinary transferrin detection and Urinary Iron levels 14
Discussion **17**
Conclusions **21**
References **22**

List of Tables and Figures

Table 1- qRT-PCR primer and reaction conditions

Figure 1- Transferrin receptor 1 (*TfR1*) and *Dmt1* mRNAs are differentially expressed in *fsn* kidney.

Figure 2- (A-C) No defect in *fsn* kidney cells to express surface Transferrin receptor 1 (TfR1) or endocytose pHrodo-Tf iron.

Figure 3- Rab7 protein, a late endosomal marker, is lower in *fsn* kidney samples.

Figure 4- PI4KIIIα mRNA levels are decreased in *fsn* kidney.

Figure 5- No difference in urine transferrin levels between *fsn* and WT mice.

Introduction

Sickle cell disease, β-thalessemia major and myelodysplastic syndrome (MDS) patients can require chronic blood transfusions, which lead to iron overloading, iron tissue deposition, and organ failure. Iron chelation therapy is the only current treatment available to decrease body iron stores. Complications associated with intravenous chelation include gastrointestinal disturbances, rash, joint pain, neutro/leucopenia, elevated serum creatinine, and decreased quality-of-life. In addition, poor compliance with chelation drugs results in increased morbidity and worse outcomes in those with iron overload. It has been estimated that up to 1 out of 3 patients prescribed intravenous chelation are non-compliant [1]. Oral chelation alternatives have improved problems with compliance, yet tolerance to the drugs and side effects still exist. Additionally, oral formulations such as deferasirox and deferiprone are significantly more expensive than the older intravenous formulation, deferoxamine. The overall costs, adverse events, complications, and decreased quality-of-life a patient endures leads to a successful treatment rate estimated at 48.8% to 63.9% with Deferasirox [1]. Therefore, there is a critical need to identify alternative methods of decreasing body iron stores in transfusion dependent diseases that will lead to better patient outcomes, improved safety, and increased compliance.

Iron transport and utilization is under control of many proteins expressed in intestine, liver, bone marrow, and other tissues. Iron transport is initiated in the intestinal lumen with the aid of apical membrane protein divalent metal transporter 1 (DMT1, gene symbol *Slc11a2*) and the ferrireductase Dcytb to move iron into enterocytes. The iron exporter ferroportin (FPN1, gene symbol, *Slc40a1*), in concert with the ferroxidase

hephaestin, transports iron across the basal membrane into the blood where it is bound by transferrin (Tf) for transport to tissues [2]. Once in circulation, transferrin-bound iron (Tf-Fe) can be utilized by many cell types expressing transferrin receptors. Transferrin receptor 1 (TfR1) is expressed on many types of human cells including basal cells of the epidermis, kidney tubular epithelium, islets of Langerhans, Küppfer cells, hepatocytes, and seminiferous tubules [3]. Tf-Fe enters these cells via clathrin-mediated endocytosis. Apical membrane receptors Megalin, Cubilin, and TfR1 have been reported to bind and internalize Tf-Fe [2]. Once internalized into endosomes and the clathrin coat is removed, the proteins DMT1, STEAP3 ferrireductase, and endosomal H^+/ATPases enable iron to dissociate from Tf and exit the endosome through DMT1 associated transport [2]. The iron can then be utilized by mitochondria to make heme, be used as a cofactor for enzymes, or stored bound to ferritin.

In the kidney, Tf-Fe is filtered in metabolically significant amounts and is normally reabsorbed in the proximal tubule [4]. Both Cubilin/Megalin and TfR1 have been observed to endocytose Tf-Fe at the proximal tubule in mice [5,6]. DMT1 has also been described to be present at the proximal tubule and thick ascending limb of rat and mouse nephron [7,8]. It is hypothesized that the proximal tubule compartment relies upon receptor-mediated endocytosis for Tf-Fe reabsorption while the later nephron relies upon DMT1 mediated iron reabsorption to capture non-protein bound iron [8,9].

Mouse models have played a critical role in understanding the mechanisms of iron transport and the flaky-skin anemia (gene symbol, *fsn*) mouse is one example. The *fsn* mouse suffers from a hereditary anemia in the homozygous condition and has the

unique ability to excrete increased levels of iron through its urine [10]. Beamer et al. demonstrated a 72-fold increase in the amount of radioactive iron (^{59}Fe) in *fsn* urine compared to wild-type (WT) controls 24 hours after oral ^{59}Fe administration [10]. The *fsn* locus has been mapped to Chromosome 17 and contains a mutation in the gene *tetratricopeptide repeat domain 7* (gene symbol, *Ttc7*) which encodes a TPR repeat domain-containing protein (TTC7) [10-12]. The mutant phenotype of *fsn* mice is caused by a 5.5 kb viral DNA ETn (early transposon) insertion which results in the addition of an in-frame exon into the final *fsn Ttc7* mRNA [11]. Recent studies in yeast, humans, and cell lines suggest that TTC7a acts as a transport protein for phosphatidylinositol 4-kinase III alpha (PI4KIIIα) to form a complex at the plasma membrane with a membrane-associated protein, Efr3b [13-16]. Avitzur et al. hypothesized that the lack of TTC7a mediated transport of PI4KIIIα to the plasma membrane resulted in decreased phosphatidylinositol 4-phosphate (PIP4) production in a human intestinal cell line (Henle-407) [15]. Numerous reports have described the importance of phosphoinositides and phosphotidylinositide kinases in the process of clathrin-mediated endocytosis [16-20]. However, the specific role of TTC7a and PI4KIIIα in iron metabolism in the kidney remains unclear.

We hypothesized that *fsn* mice have the ability to excrete high levels of iron in their urine due to defects in transferrin receptor mediated endocytosis in the kidney. The *fsn Ttc7* mutation, which results in an elongated TTC7 protein, may be unable to transport PI4KIIIα to the plasma membrane effectively [11]. As a result, PI4KIIIα cannot function properly at the plasma membrane to maintain PIP4 levels. Alterations in phosphoinositide pools can have detrimental effects on endocytosis and downstream

signaling. Our aim was to characterize adult *fsn* mouse for renal transferrin endocytosis using flow cytometry, renal iron transport gene expression utilizing quantitative real-time PCR, and urinary iron loss via a transferrin ELISA and non-heme iron assay. This study would further elucidate the relationship of TTC7a and PI4KIIIα in renal iron reabsorption of *fsn* anemia mouse mutant.

Methods

Ethics Statement

Animal care and procedures were in accordance with institutional guidelines. This study was conducted under approval of University of Missouri at Kansas City IACUC and IBC (Protocol # 1214).

Mice

BALB/cJ-+/*fsn* mice were originally obtained from The Jackson Laboratory (Bar Harbor, ME). BALB/cJ-*fsn*/*fsn* mice were produced by mating BALB/cJ-+/*fsn* carrier mice. PCR genotyping was done to confirm homozygosity for the *fsn Ttc7* mutation using primers specific to the Etn and *Ttc7* sequence. By weaning age (21 days), the *fsn* phenotype is obvious with patchy flaky skin, hunched posture, and runted stature. WT and *fsn* littermates were housed at the University of Missouri at Kansas City Laboratory Animal Research Core facility.

High Iron Diet

A high iron diet (2% wt/wt Carbonyl Iron supplemented in Harlen Teklad 2018 Rodent Diet) was purchased from Harlen Teklad (Madison, WI). For high iron diet experiments, *fsn* and WT littermates were fed the high iron diet starting at 5 weeks of age as previously described for 4 weeks [12].

Quantitative Real-Time PCR (qRT-PCR)

WT and *fsn* kidneys were used to extract RNA using RNeasy Midi kit (Qiagen Inc., Valencia, CA) according to manufacturer's protocol. Quality of RNA and concentration was measured using agarose gel electrophoresis and spectrophotometry (NanoDrop2000). cDNA was synthesized from 500ng kidney RNA samples using

qScript cDNA SuperMix (Quanta Biosciences, Gaithersburg, MD). qRT-PCR was performed using PerfeCta Sybr Green FastMix (Quanta Biosciences, Gaithersburg, MD) on CFX Connect® qRT-PCR system (Bio-Rad Laboratories, Hercules, CA). All analysis was done on duplicate samples using the ΔΔCt method [21]. Internal controls were used and HPRT was used as the housekeeping gene. qRT-PCR primers were designed through IdtDNA PrimerQuest. All primers were optimized to at least 97% efficiency using standard curves of serial dilutions of the qRT-PCR reactions. All primers and reaction conditions are compiled in Table 1.

Gene	Sequence	Final Concentration (nM)	Annealing Temperature (°C)
Cubilin	F- CAGTCCTGGCTCCTTGATAAC R- GGAAAGGACCATCTCGAATCTC	100	60
Dmt1	F- GGGTTGGCAGTGTTTGATTG R- CTGGGCTGTTAGTCATCTGG	300	60
Fpn1	F- CTGGATTGTTGTTGTGGCAG R- CCAGGATGTTGGTTAGCTGG	300	60
HPRT	F-TGGTGGAGATGATCTCTCAACTTT R-CCAGTGTCAATTATATCTTCCACAA	400	60
Megalin	F- CCTTGCACAGACACCGAATA R- CTCCACAGTCGTCCACATTATC	100	60
PIP5Kg	F- GGAGTGCCCATCCTGTATTT R- TTCTGTGTCTTGTCGTCTTTCT	100	60
Steap3	F- CTGCTCAGCTTCTTCTTCGC R- TGCTTCACAGCCAGATTGAC	300	60
TfR1	F-GTCCAGTGTGGGAACAGGTC R-CAGTCCAGCTGGCAAAGATT	300	60
PI4KIIIa	F- GCTGGGAACCAGACATCAA R- GATAACCTCGGACACACATCTC	100	58
PIP5Ka	F- GGAGAAAGGCTCCTGCTTTAT R- GACCAGTGCTTTCCAAGAGT	300	58
Efr3b	F- CACCTGTGGCAGTCTTCTATG R- GGCACCAACCACAGCTAATA	300	58
PIP5Kb	F- CCTGAAAGGCTCCACATACAA R- CAGGAAGTCCAGGTCCTTAAAC	300	56

Table 1. qRT-PCR primers and reaction conditions.

Flow cytometry

fsn and WT littermate kidneys were dissected and made into single cell suspensions by cutting into pieces followed by successive needle aspirations (16G-20G) in ice-cold 1X RPMI-1640 (Cellgro, Mediatech Inc., Manassas, VA). The cell suspensions were washed with ice-cold 1X RPMI-1640 and resuspended in the corresponding cocktail of either pHrodo Red-Transferrin (pHrodo-Tf) (Life Technologies, Grand Island, NY) or Transferrin Receptor 1-FITC (TfR1-FITC) or Rat IgG2ak-FITC (isotype-FITC) (Affymetrix eBioscience, San Diego, CA) in FluoroBrite 1X DMEM (Life Technologies, Grand Island, NY) supplemented with 25mM HEPES and 1% bovine serum albumin. pHrodo-Tf labeled samples were incubated for 20 minutes at 37°C while the TfR1-FITC and isotype-FITC labeled samples were incubated on ice for 45 minutes. Samples were then washed with ice-cold FluoroBrite DMEM (25mM HEPES, 1% BSA). Samples were run on BD LSRII flow cytometer (KUMed Flow Core). All analysis was done using FlowJo software (Tree Star Inc., Ashland, OR) gating on live cells and excluding doublets. Gating was based on unstained and isotype controls.

Western Blot of kidney samples and Antibodies

fsn and WT littermate kidney was dissected after 4 weeks on a high iron diet. Half of the kidney was used for protein extraction and other half for mRNA extraction described above. NP-40 cell lysis buffer with protease and phosphatase inhibitors (100X Halt™ Protease & Phosphatase Inhibitor Cocktail, Sigma-Aldrich, St. Louis, MO) were used to extract whole protein from kidney samples. Quantification of protein levels was

done via the BCA Protein Assay kit (Pierce™ Thermo Scientific, Waltham, MA). 20ug of total protein was loaded per sample on 4-15% TGX mini Protean gels (Bio-Rad Laboratories, Hercules, CA) and subjected to SDS-PAGE. Immunoblotting was performed with the following antibodies: Rabbit α-Rab5 mAb, Rabbit α-Rab7 mAb, Rabbit α-Rab11 mAb (Cell Signaling Technology Inc., Danvers, MA), and rabbit mAb-HRP β-Actin (Cell Signaling Technology Inc., Danvers, MA). Secondary antibody used was α-Rabbit-Horseradish Peroxidase (Cell Signaling Technology Inc., Danvers, MA). Results were visualized by chemiluminescence, exposure on radiographic film, and band intensity was measured with UVP imaging system (UVP, LLC, Upland, CA). Densitometry was calculated with VisionWorksLS Analysis Software (UVP, LLC, Upland, CA). Relative band intensity was calculated by dividing each sample's band intensity by its β-Actin loading control band intensity.

Transferrin ELISA and Iron Measurement in Urine Samples

After 3 weeks on the high iron diet, urine was collected at least 2 times a day for 7 days from *fsn* and WT littermates by manual collection. Urine was pooled for each mouse and transferrin was measured with a mouse transferrin ELISA kit according to manufacturer's protocol (GenWay BioTech Inc., San Diego, CA). Urine creatinine was measured at Children's Mercy Hospital Kansas City's Clinical Chemistry and Toxicology Laboratory per manufacturer's protocol (CREA Slides, VITROS Chemistry Products, Ortho-Clinical Diagnostics, Inc., Rochester, NY) and was used to standardize transferrin urine levels. Iron urine levels was measured as previously described in serum [12].

Urine Electrophoresis

10 ul undiluted urine samples collected from WT and *fsn* mice on a high iron diet, as described above, were loaded 1:1 with laemmeli buffer on 4-15% TGX mini Protean gels (Bio-Rad Laboratories, Hercules, CA) and subjected to SDS-PAGE. Samples collected from mice on a normal diet were pooled from several mice and 10 ul was loaded for *fsn* and WT as described above. Total protein was resolved with Bio-Safe Coomassie (Bio-Rad Laboratories, Hercules, CA) per manufacturer's protocol. Image was taken on UVP imaging system (UVP, LLC, Upland, CA).

Statistics

Two-sided Student's t-test was used to compare means assuming unequal variance. All bar graphs represent means with standard error of the mean (SEM) error bars. Statistical significance was set at $p<0.05$.

Results

Iron transport gene expression

In order to determine whether the *fsn Ttc7* mutation has an effect on iron transport gene expression, qRT-PCR was performed in whole kidney mRNA samples from *fsn/fsn* (*fsn,* n=5) or wild-type (WT, n=3) littermates. Our results demonstrate that transferrin receptor 1 (*TfR1*) mRNA expression was increased 1.77 fold (p=0.02) in kidney from *fsn* mice when compared to WT littermates at 5 weeks of age (Figure 1). Also, divalent metal transporter 1 (*Dmt1*) mRNA expression was nearly 2 fold (p=0.003) lower in *fsn* kidney compared to WT littermates (Figure 1). No changes were observed in Ferroportin (*Fpn1*) and Six-transmembrane epithelial antigen of the prostate (*Steap3*) expression in *fsn* and WT kidney at 5 weeks of age (Figure 1).

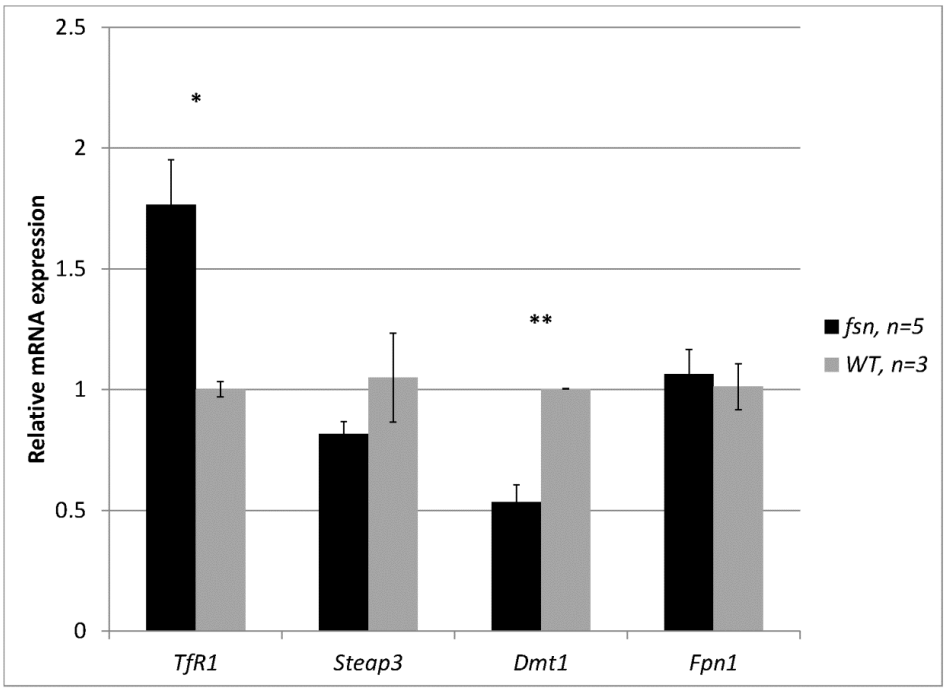

Figure 1. Transferrin receptor 1 (*TfR1*) and *Dmt1* mRNAs are differentially expressed in *fsn* kidney. mRNA from *fsn/fsn* (*fsn*) or wild-type (WT) littermates was used to measure gene expression in whole kidney. Black (*fsn*) and grey (WT) bars represent mean relative mRNA expression +/- SEM error bars. Statistical significance indicated by * = $p<0.05$, ** = $p<0.01$.

Transferrin receptor 1 & Transferrin uptake flow cytometry

Given the increased mRNA levels of *TfR1*, we sought to determine the surface protein expression of TfR1 in single cell suspensions of whole kidney from *fsn* (n=5) and WT (n=6) littermates. Our results show 15.6% of TfR1 positive kidney cells in *fsn* ($p<0.01$) versus 4.41% TfR1 positive in WT or heterozygous littermates (Figure 2a & 2b). This data corroborates with the increase in the *TfR1* expression observed in *fsn* kidney (Figure 1).

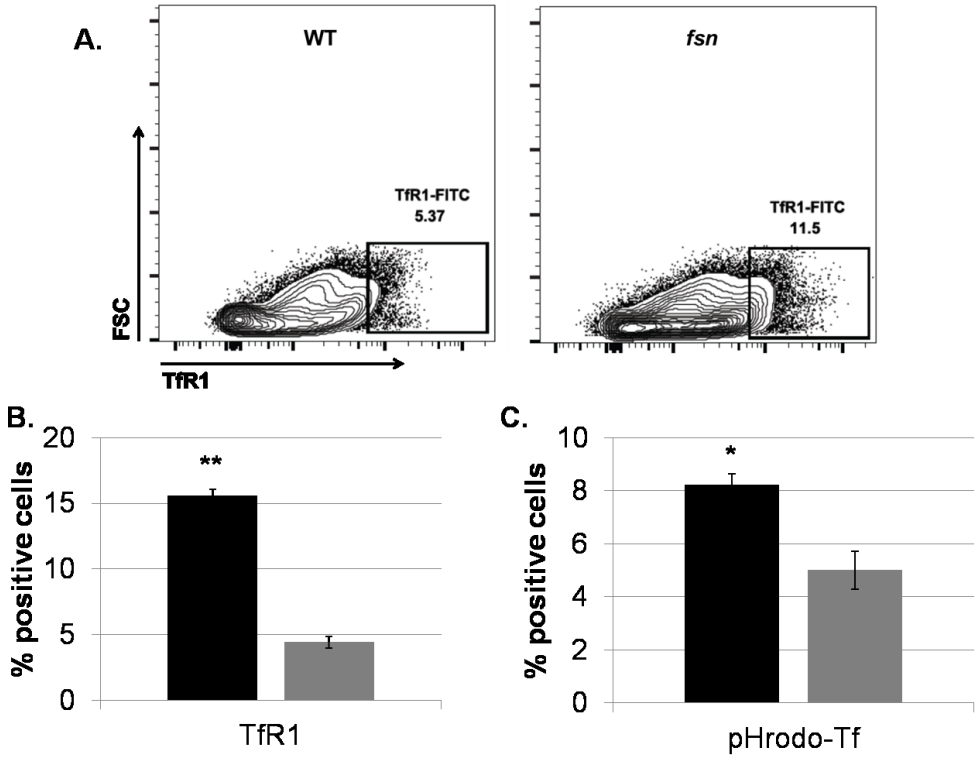

Figure 2. No defect in *fsn* kidney cells to express surface Transferrin receptor 1 (TfR1) or endocytose pHrodo-Tf iron. Single cell kidney suspensions from *fsn/fsn* (*fsn*) or wild-type (WT) littermates were used to measure the (A & B) percentage of TfR1+ cells (n=5, n=6) and (C) pHrodo-Tf uptake *in vitro* (n=3, n=3). Black (*fsn*) and grey (WT) bars represent (B) mean % TfR1+ or (C) mean % pHrodo-Tf+. Statistical significance indicated by * = $p<0.05$, ** = $p<0.01$.

The increased level of *TfR1* mRNA and the increased population of TfR1-positive cells is *fsn* mice led us to determine whether transferrin receptor-mediated endocytosis was impaired in *fsn* kidney cells. The ability of *fsn* and WT kidney cells to endocytose pHrodo Red-Transferrin (pHrodo-Tf), a pH-sensitive fluorescent dye bound to human transferrin, was measured. Surprisingly, the *fsn* kidney cells (n=3) showed 8.24% pHrodo-Tf positive cells compared to 5.01% pHrodo-Tf positive cells in WT (n=3) samples (p=0.027, Figure 2c). These data suggest there is no defect in *fsn* kidney cells to internalize Tf-Fe when compared to WT mouse kidney cells. Given the pHrodo-Tf requires an acidic environment to fluoresce at maximal intensity; the *fsn* mice do not display an obvious defect in acidification of endosomal compartments with this assay.

Endosomal protein markers in the kidney

Tf and TfR1 are processed through endosomes and recycled to the plasma membrane. To determine if endosomal trafficking in *fsn* kidney cells was intact, the protein levels of known endosomal proteins were measured. Kidneys were dissected from *fsn* (n=3) and WT (n=2) mice placed on a high iron diet (2% wt/wt) and used for protein extraction. No difference in endosomal Rab5 and Rab11 protein levels was observed between *fsn* and WT kidney protein lysates (Figure 3b). However, Rab5 protein levels had a trend of being higher in *fsn* samples compared to WT, p=0.08 (Figure 3b). The endosomal Rab7 protein level was 20% lower in *fsn* kidney samples at 9 weeks of age compared to WT, p=0.007 (Figure 3b).

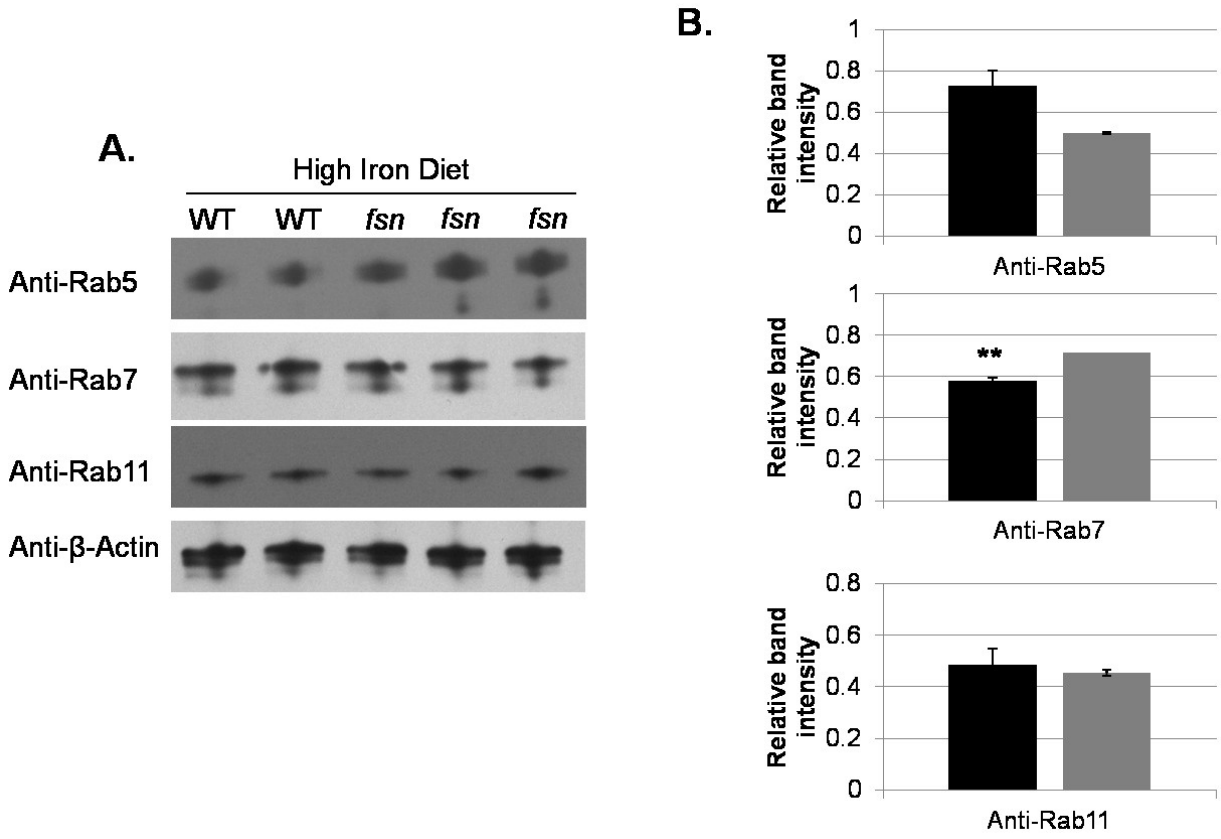

Figure 3. Rab7 protein, a late endosomal marker, is lower in *fsn* kidney samples. Kidney protein lysates were resolved via SDS-PAGE and immunoblotting from 9 week old *fsn* and WT mice on a high iron diet for 4 weeks. B.) Bar graphs represent mean relative band intensity for *fsn* (black, n=3) and WT (grey, n=2) +/- SEM error bars. Statistical significance indicated by * = $p<0.05$, ** = $p<0.01$.

qRT-PCR on TTC7a and Transferrin endocytosis related genes

To determine the relative gene expression of the recently identified protein partners of TTC7a and transferrin endocytosis genes [4-6,14,15], quantitative real-time PCR (qRT-PCR) was utilized. Our results demonstrate that Megalin and Cubilin mRNA levels had a trend of being lower in *fsn* kidney when compared to WT, however, they were not statistically significant differences (Figure 4). Phosphatidylinositol 5-phosphate Kinase (PIP5K) isoforms and EfR3b did not show any significant differences between *fsn* and WT kidney samples (Figure 4). Interestingly, phosphatidylinositol 4-kinase III

alpha (PI4KIIIα) expression was decreased 36% in the *fsn* samples (n=5) compared to WT (n=3) samples (p=0.027, Figure 4). This data corroborates recent data demonstrating decreased PI4KIIIα protein by western blot in the human Henle-407 intestinal cell line lentivirally infected with TTC7a shRNAs [15].

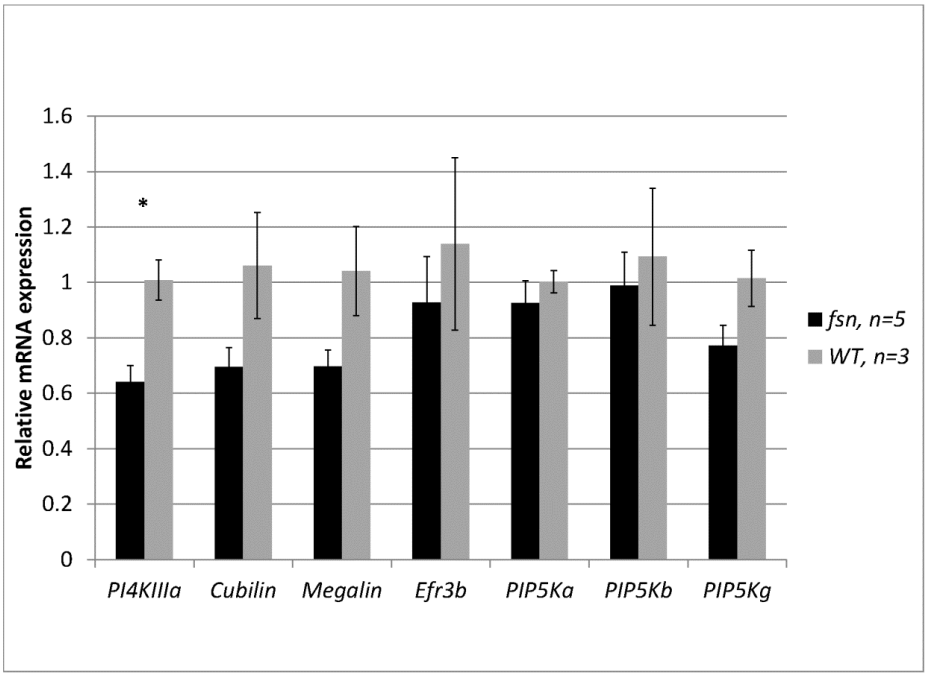

Figure 4. PI4KIIIα mRNA levels are decreased in *fsn* kidney. mRNA from *fsn/fsn* (*fsn*) or wild-type (WT) littermates was used to measure gene expression in whole kidney. Black (*fsn*) and grey (WT) bars represent mean relative expression +/- SEM error bars. Statistical significance indicated by * = p<0.05.

Urinary transferrin detection and Urinary Iron levels

In order to determine if the urinary iron loss observed in *fsn* mice was related to transferrin bound iron excretion, we utilized a transferrin ELISA to measure urinary transferrin concentration. If our pHrodo-Tf assay is not sensitive enough to detect a defect in Tf-Fe uptake, the *fsn* urine samples should still contain higher levels of transferrin by this assay. WT (n=3) and *fsn* (n=3) mice were fed a high iron diet for 3

weeks and urine was collected daily for 7 days. Urine transferrin levels, as well as, urine non-heme iron levels were measured.

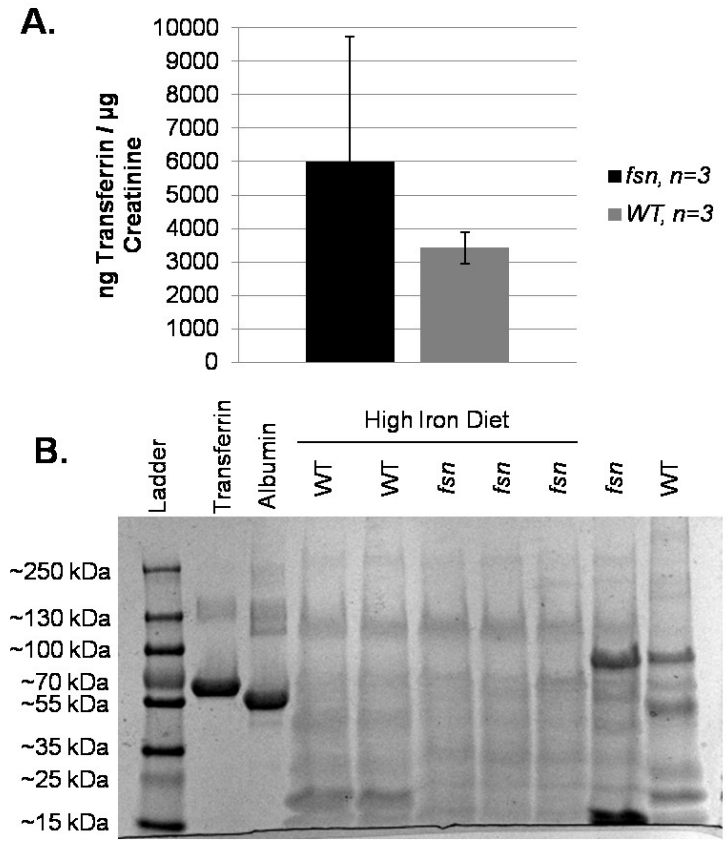

Figure 5. No difference in urine transferrin levels between *fsn* and WT mice. A.) Urine was collected from *fsn/fsn* (*fsn*) and WT mice for 7 days after 3 weeks on a high iron diet. Black (*fsn*) and grey (WT) bars represent mean ng of transferrin per ug creatinine +/- SEM error bars. B.) Urine total protein resolved with Coomassie stain.10ul of urine loaded per sample onto Tris-Glycine SDS-PAGE gel. 10ug of mouse apo-transferrin and bovine serum albumin loaded as control samples. The *fsn* and WT samples on normal diet (no bar) were pooled from several mice at 5 weeks of age.

Our results indicate that *fsn* mice do not have a significantly higher level of transferrin in their urine when compared to WT littermates (p=0.35, Figure 5A). Additionally, the mean iron concentration detected in *fsn* (n=2) samples was 36.5 µg/dl while the WT (n=3) urine samples were below the level of detection for the assay (<10 µg/dl). It was further determined via urine electrophoresis that there was no gross proteinuria in the *fsn* urine samples versus WT (Figure 5B). However, some differential

banding was noted between WT and *fsn* samples on the high iron diet, as well as, between the normal diet and high iron diet urine samples. These data suggest that the acute urinary iron loss observed in *fsn* mice is not due solely to transferrin-bound iron excretion.

Discussion

The current treatment for many blood transfusion-dependent patients experiencing iron overload is chelation. Intravenous chelation drugs have been the standard of care for reducing body iron stores. However, this approach has adverse effects including liver, kidney, visual and auditory toxicity, joint pain, and even death. Not every individual requiring chelation can tolerate treatment and there is currently a lack of alternative pharmaceuticals. The *fsn* mouse suffers from an iron deficiency anemia that is believed to be the result of defective iron metabolism [10-12]. Over 6 weeks of life the serum iron levels decline in *fsn* mice compared to WT littermates whom accrue iron in the serum [12]. Additionally, it has been observed that *fsn* mice excrete high levels of iron in their urine after oral ^{59}Fe administration compared to WT mice [10]. We set out to identify the mechanism by which *fsn* mice are able to excrete elevated iron in their urine. Further characterizing the defect in *fsn* mouse kidney could lead to the identification of pharmaceutical targets that modulate body iron storage, treating iron overload disorders.

Experiments were designed to identify whether known iron metabolism and transport genes were differentially expressed in *fsn* kidney compared to wild-type (WT). We found that *Steap3*, a ferrireductase, and *Fpn1* mRNA expression was not different between *fsn* and WT kidney samples at 5 weeks of age (Figure 1). Interestingly, our data demonstrates that *TfR1* and *Dmt1* mRNA expression was differentially expressed in *fsn* mouse kidney samples at 5 weeks of age (Figure 1). *TfR1* mRNA levels were 1.77 fold higher while *Dmt1* mRNA was nearly 2 fold lower in *fsn* samples when compared to WT (Figure 1). Further, our goal was to determine if this increase in *TfR1*

mRNA would translate into increased TfR1 protein levels in the kidney of *fsn* mice. Our data exhibited a 3.5 fold higher percentage of TfR1 positive cells in *fsn* kidney by flow cytometry compared to WT (Figure 2a, 2b).

In order to identify if the observed *TfR1* gene and protein expression increase was in compensation for a defect in TfR1 endocytosis, we aimed to verify whether single cell suspensions of *fsn* kidney cells were capable of endocytosing a pH-sensitive dye labeled transferrin (pHrodo-Tf) molecule (Figure 2c). This assay is based on the principle that the pHrodo-Tf bound by TfR1 is internalized through clathrin-mediated endocytosis (Life Technologies, Grand Island, NY). Upon internalization and acidification of the endosome the pHrodo-Tf molecule fluoresces, allowing detection via flow cytometry. We observed that *fsn* kidney cells are capable of endocytosing pHrodo-Tf (Figure 2c). This suggests that the TfR1 protein expression increase is not a result of a defect of TfR1 internalization and endosomal acidification. We speculated that the increased TfR1 mRNA and percent TfR1-positive cells in *fsn* kidney was related to the low iron status of these mice. TfR1 mRNA is known to contain iron response elements (IRE) which result in protection of the mRNA from degradation during low cellular iron levels [22-26]. However, the increased TfR1 mRNA and protein we observed suggested a compensatory effect as a result of a defect in downstream TfR1 endosomal trafficking and recycling.

We measured the amount of endosomal Rab small GTPases by western blot in *fsn* and WT kidney to detect any difference in protein levels which could indicate endosomal trafficking dysfunction. Rab5, Rab7, and Rab11 are associated with

early/sorting, late, and recycling endosomes, respectively [27]. Our data showed that Rab5 and Rab11 protein levels were not statistically different in *fsn* kidney protein samples when compared to WT kidneys at 9 weeks of age though Rab5 protein had a trend of being higher in *fsn* kidney (Figure 3b). However, Rab7 protein levels were found to be 20% lower in the *fsn* kidney (Figure 3b). This suggests that there may be a defect in the processing of late endosomes or the transition from early endosomes. Rab7 has classically been described as a late endosomal marker, however, recently it was shown to be required for early endosomal maturation events of low density lipoproteins [28]. siRab7 depletion led to a modest reduction in surface transferrin receptor or transferrin surface binding in Hela cells [28]. Girard et al. concluded that Rab7 in Hela cells had little impact on transferrin receptor recycling [28]. This is contrary to our results showing an increased percentage of surface transferrin receptor positive cells and modest increase internalization of fluorescent transferrin in *fsn* kidney cells (Figure 2). The observed differences could be species specific as Girard et al. utilized a Hela cell line. However, we speculated that the decreased Rab7 protein level in *fsn* kidney is not responsible for the increased urinary iron excretion in *fsn* mice.

In order to rule out changes in gene expression of other known transferrin binding proteins in the kidney, qRT-PCR was utilized. Cubilin and Megalin are known to work in concert to bind and internalize many proteins filtered by the glomerulus including IgA, intrinsic factor, albumin and transferrin [5,6,29-31]. However, our data did not detect a statistically significant difference in *Cubilin* or *Megalin* mRNA (Figure 4). Furthermore, our study assessed whether PIP5K mRNA levels, which are downstream of PI4KIIIα in the phosphotidylinositide cascade, were elevated to determine if a defect

in TTC7 (which is reported to affect PI4KIIIα localization) would result in PIP5K gene compensation. Our data did not demonstrate a difference in any of the three PIP5K isoform's mRNA comparing *fsn* and WT 5 week old kidney samples indicating *fsn* kidney cells are not compensating with PIP5K gene expression (Figure 4). It was found; however, that PI4KIIIα mRNA levels were significantly lower in *fsn* samples (Figure 4). This corroborates a previous report demonstrating lower PI4KIIIα protein levels in human Henle-407 intestinal cells treated with lentiviral Ttc7a-shRNA particles [15]. Decreased PI4KIIIα at the membrane of *fsn* kidney cells could impact the ability to signal through PIP2 via secondary messengers diacylglycerol (DAG) and Ins(1,4,5)P3. As Bojjireddy et al. demonstrated after chemical inhibition of PI4KIIIα, strong phospholipase C stimulation led to PIP2 depletion in HEK293 cells [32].

We aimed to determine if the excess iron loss previously reported in the urine of *fsn* mice could be explained by urinary loss of transferrin bound iron [10]. Our data showed no difference in transferrin levels in the urine of *fsn* mice when compared to WT littermates though there was wide variability in the *fsn* samples (Figure 5a). This suggests that the excess iron excretion found in *fsn* urine in this study is not due to excess transferrin-bound iron loss. This also supports our observation that there is no defect in surface transferrin receptor expression or ability to internalize transferrin-bound iron in the *fsn* kidney (Figure 2). Additionally, our data suggests no difference in mRNA levels of the known transferrin binding receptors Cubilin or Megalin in the *fsn* kidney (Figure 4). Urine electrophoresis of *fsn* and WT samples placed on a normal diet or high iron diet did resolve differential protein patterns.

These results suggest that the *fsn* kidney is capable of endocytosing transferrin-bound iron and the previously reported acute urinary iron loss is not due to gross transferrin-bound iron excretion. The possibility cannot be ruled out that iron is being filtered through the glomerulus bound to other protein partners (ferritin, albumin, lipocalin etc.) or as free iron (Fe^{2+} or Fe^{3+}). We suggest further investigation into the protein levels of DMT1 in the kidney of *fsn* mice. A deficiency of this critical iron transport protein could explain the urinary iron loss observed in *fsn* urine. It is important to note that known mouse and rat models containing mutated *Dmt1* genes have been reported to excrete high levels of iron and transferrin in urine [7,33]. However, the Belgrade rat exhibits a renal developmental abnormality with lower glomeruli number compared to WT rats [7]. This is hypothesized to result in the observed progressive renal fibrosis and sclerosis. *fsn* mice could possess a condition in which there is a decrease in DMT1 protein that results in urinary iron loss without renal developmental issues. *fsn* mice have not been reported to have developmental kidney issues yet have been reported to have glomerular thickening and immune complex deposition in the mesangium as early as 4 weeks old [34].

Conclusions

We have demonstrated that the *fsn* mouse kidney is not defective in internalizing transferrin-bound iron and urinary iron excretion cannot be explained by transferrin-bound iron leak. Further work should aim to identify the role of DMT1 protein in iron absorption in the nephron of *fsn* mice. We have demonstrated a lower *Dmt1* mRNA level and this could reflect a decrease of apical DMT1 responsible for renal iron reabsorption.

References

1. Vanorden HE, Hagemann TM (2006) Deferasirox--an oral agent for chronic iron overload. Ann Pharmacother 40: 1110-1117.
2. Garrick MD, Garrick LM (2009) Cellular iron transport. Biochim Biophys Acta 1790: 309-325.
3. Gatter KC, Brown G, Trowbridge IS, Woolston RE, Mason DY (1983) Transferrin receptors in human tissues: their distribution and possible clinical relevance. J Clin Pathol 36: 539-545.
4. Zhang D, Meyron-Holtz E, Rouault TA (2007) Renal iron metabolism: transferrin iron delivery and the role of iron regulatory proteins. J Am Soc Nephrol 18: 401-406.
5. Kozyraki R, Fyfe J, Verroust PJ, Jacobsen C, Dautry-Varsat A, et al. (2001) Megalin-dependent cubilin-mediated endocytosis is a major pathway for the apical uptake of transferrin in polarized epithelia. Proc Natl Acad Sci U S A 98: 12491-12496.
6. Weyer K, Storm T, Shan J, Vainio S, Kozyraki R, et al. (2011) Mouse model of proximal tubule endocytic dysfunction. Nephrol Dial Transplant 26: 3446-3451.
7. Veuthey T, Wessling-Resnick M (2014) Pathophysiology of the Belgrade rat. Front Pharmacol 5: 1-13.
8. Moulouel B, Houamel D, Delaby C, Tchernitchko D, Vaulont S, et al. (2013) Hepcidin regulates intrarenal iron handling at the distal nephron. Kidney Int 84: 756-766.
9. Smith CP, Thevenod F (2009) Iron transport and the kidney. Biochim Biophys Acta 1790: 724-730.
10. Beamer WG, Pelsue SC, Shultz LD, Sundberg JP, Barker JE (1995) The Flaky Skin mutation mice Map location and description of the anemia. Blood 86: 3220-3226.
11. White RA, McNulty SG, Nsumu NN, Boydston LA, Brewer BP, et al. (2005) Positional cloning of the Ttc7 gene required for normal iron homeostasis and mutated in hea and fsn anemia mice. Genomics 85: 330-337.
12. White RA, McNulty SG, Roman S, Garg U, Wirtz E, et al. (2004) Chromosomal localization, hematologic characterization, and iron metabolism of the hereditary erythroblastic anemia (hea) mutant mouse. Blood 104: 1511-1518.
13. Wu X, Chi RJ, Baskin JM, Lucast L, Burd CG, et al. (2014) Structural insights into assembly and regulation of the plasma membrane phosphatidylinositol 4-kinase complex. Dev Cell 28: 19-29.
14. Baird D, Stefan C, Audhya A, Weys S, Emr SD (2008) Assembly of the PtdIns 4-kinase Stt4 complex at the plasma membrane requires Ypp1 and Efr3. J Cell Biol 183: 1061-1074.
15. Avitzur Y, Guo C, Mastropaolo LA, Bahrami E, Chen H, et al. (2014) Mutations in Tetratricopeptide Repeat Domain 7A Result in a Severe Form of Very Early Onset Inflammatory Bowel Disease. Gastroenterology 146: 1028-1039.
16. Nakatsu F, Baskin JM, Chung J, Tanner LB, Shui G, et al. (2012) PtdIns4P synthesis by PI4KIIIalpha at the plasma membrane and its impact on plasma membrane identity. J Cell Biol 199: 1003-1016.
17. Spiro DJ, Boll W, Kirchhausen T, Wessling-Resnick M (1996) Wortmannin alters the transferrin receptor endocytic pathway in vivo and in vitro. Mol Biol Cell 7: 355-367.
18. Shpetner H, Joly M, Hartley D, Corvera S (1996) Potential Sites of PI-3 Kinase Function in the Endocytic Pathway Revealed by The PI-3 Kinase Inhibitor, Wortmannin. The Journal of Cell Biology 132: 595-605.
19. Abe N, Inoue T, Galvez T, Klein L, Meyer T (2008) Dissecting the role of PtdIns(4,5)P2 in endocytosis and recycling of the transferrin receptor. J Cell Sci 121: 1488-1494.
20. van den Bout I, Divecha N (2009) PIP5K-driven PtdIns(4,5)*P*2 synthesis:regulation and cellular functions. Journal of Cell Science 122: 3837-3850.
21. Pfaffl MW (2001) A new mathematical model for relative quantification in real-time RT-PCR. Nucleic Acids Res 29: e45.

22. Mullner EW, Kuhn LC (1988) A stem-loop in the 3' untranslated region mediates iron-dependent regulation of transferrin receptor mRNA stability in the cytoplasm. Cell 53: 815-825.
23. Mullner EW, Neupert B, Kuhn LC (1989) A specific mRNA binding factor regulates the iron-dependent stability of cytoplasmic transferrin receptor mRNA. Cell 58: 373-382.
24. Casey JL, Di Jeso B, Rao K, Rouault TA, Klausner RD, et al. (1988) The promoter region of the human transferrin receptor gene. Ann N Y Acad Sci 526: 54-64.
25. Casey JL, Hentze MW, Koeller DM, Caughman SW, Rouault TA, et al. (1988) Iron-responsive elements: regulatory RNA sequences that control mRNA levels and translation. Science 240: 924-928.
26. Koeller DM, Casey JL, Hentze MW, Gerhardt EM, Chan LN, et al. (1989) A cytosolic protein binds to structural elements within the iron regulatory region of the transferrin receptor mRNA. Proc Natl Acad Sci U S A 86: 3574-3578.
27. Clague MJ (1998) Molecular aspects of the endocytic pathway. Biochem J 336 (Pt 2): 271-282.
28. Girard E, Chmiest D, Fournier N, Johannes L, Paul JL, et al. (2014) Rab7 is functionally required for selective cargo sorting at the early endosome. Traffic 15: 309-326.
29. Amsellem S, Gburek J, Hamard G, Nielsen R, Willnow TE, et al. (2010) Cubilin is essential for albumin reabsorption in the renal proximal tubule. J Am Soc Nephrol 21: 1859-1867.
30. Christensen EI, Nielsen R, Birn H (2013) From bowel to kidneys: the role of cubilin in physiology and disease. Nephrol Dial Transplant 28: 274-281.
31. Christensen EI, Verroust PJ, Nielsen R (2009) Receptor-mediated endocytosis in renal proximal tubule. Pflugers Arch 458: 1039-1048.
32. Bojjireddy N, Botyanszki J, Hammond G, Creech D, Peterson R, et al. (2014) Pharmacological and genetic targeting of the PI4KA enzyme reveals its important role in maintaining plasma membrane phosphatidylinositol 4-phosphate and phosphatidylinositol 4,5-bisphosphate levels. J Biol Chem 289: 6120-6132.
33. Canonne-Hergaux F, Gros P (2002) Expression of the iron transporter DMT1 in kidney from normal and anemic mk mice. Kidney Int 62: 147-156.
34. Sundberg JP, France M, Boggess D, Sundberg BA, Jenson AB, et al. (1997) Development and progression of psoriasiform dermatitis and systemic lesions in the flaky skin (fsn) mouse mutant. Pathobiology 65: 271-286.